





Article

Study of the Applicability of Thermochemical Processes for Solid Recovered Fuel

Juan Jesús de la Torre-Bayo ¹, Montserrat Zamorano ¹ , Juan Carlos Torres-Rojo ², Noemí Gil-Lalaguna ³ , Gloria Gea ³, Isabel Fonts ³  and Jaime Martín-Pascual ^{1,*} 

¹ Department of Civil Engineering, University of Granada, 18071 Granada, Spain; juanjebdm@ugr.es (J.J.d.I.T.-B.); zamorano@ugr.es (M.Z.)

² Emasagra S.A., 18009 Granada, Spain; jctorres@emasagra.es

³ Thermochemical Processes Group, Aragon Institute of Engineering Research (I3A), University of Zaragoza, 50009 Zaragoza, Spain; noemigil@unizar.es (N.G.-L.); glogea@unizar.es (G.G.); isabelfo@unizar.es (I.F.)

* Correspondence: jmpascual@ugr.es; Tel.: +34-958246142

Abstract: Within the context of the new circular model for wastewater treatment aimed at achieving zero waste, this research seeks an alternative to landfill disposal of waste screenings. It examines the feasibility of thermochemical processes—combustion and gasification—for the valorisation of solid recovered fuel (SRF) derived from screening wastes, which are the only waste in wastewater treatment plants (WWTPs) that typically have an absence of existing recycling or valorisation processes. Laboratory-scale experiments assessed the technical viability of gasification, and energy balances were calculated for both combustion and the syngas obtained from gasification experiments. Results indicate that both processes are feasible for SRF valorisation. Combustion demonstrated the highest energy efficiency, yielding up to 1.6 MJ per kg of raw SRF, compared to gasification's maximum of 1.4 MJ. The moisture content in SRF feedstock influences both processes, underscoring the need to optimise moisture levels. Additionally, combustion showed a higher conversion efficiency due to the complete oxidation of the feedstock, whereas gasification produced valuable syngas that can be further utilised for energy production or as a chemical feedstock. The study concludes that, from a purely energetic perspective, combustion is the most efficient process for SRF valorisation. However, gasification offers significant environmental and sustainability advantages, including lower greenhouse gas emissions and the potential for integrating with renewable energy systems, making it a more attractive option for long-term sustainability goals.

Keywords: screening waste; wastewater treatment plants; solid recovered fuel; waste-to-energy; thermochemical process; gasification; combustion



Citation: de la Torre-Bayo, J.J.; Zamorano, M.; Torres-Rojo, J.C.; Gil-Lalaguna, N.; Gea, G.; Fonts, I.; Martín-Pascual, J. Study of the Applicability of Thermochemical Processes for Solid Recovered Fuel. *Appl. Sci.* **2024**, *14*, 10765. <https://doi.org/10.3390/app142210765>

Academic Editors: Janusz Lasek, Chao-Wei Huang and Yueh-Heng Li

Received: 24 September 2024
Revised: 12 November 2024
Accepted: 15 November 2024
Published: 20 November 2024



Copyright: © 2024 by the authors. Licensee MDPI, Basel, Switzerland. This article is an open access article distributed under the terms and conditions of the Creative Commons Attribution (CC BY) license (<https://creativecommons.org/licenses/by/4.0/>).

1. Introduction

The operation of wastewater treatment plants (WWTPs) generates waste streams of various compositions and characteristics, such as sands, oils and, sludge [1]. In the realm of waste management, recycling or energy recovery processes are commonly implemented for a vast majority of these waste streams [2]. Nevertheless, a notable exception pertains to screening waste, which, along with digestate derived from anaerobic digestion, typically remains inadequately addressed [3]. The achievement of “zero waste” in WWTPs requires the valorisation of the screening waste, which continues to be disposed of in landfills [4].

Most studies on the treatment of this waste have focused on anaerobic digestion. Methane yields reported range from 0.19 [5] to 1.04 CH₄/g VS [4], suggesting that screening residues could serve as a potential energy source [6]. However, challenges have been noted in the process due to the presence of plastics and textiles [7], as well as low methane production yields, which would require higher biomass concentrations [4]. These issues could render this solution economically unviable [8], unless existing sludge digesters were adapted for co-digestion [9]. The composition of the screening can be equated to that

of other municipal solid wastes (MSWs) as rejects from mechanical biological treatment (MBT) plants [10]. Similar to screening waste, these rejects consist primarily of fractions such as paper and cardboard, plastics, and organic matter [11]. These rejects already have established energy recovery treatments, such as the production of solid recovered fuel (SRF) to be used in thermochemical processes [12]. In addition, the latest update of the ISO 21640:2021 [13] considers solid waste from urban wastewater treatment as a possible origin for SRF production [13]. The technical feasibility of this process was demonstrated in a laboratory-scale project in Granada, Spain [14]: both a non-densified and a densified SRF [15] were produced from the screening waste from a WWTP (called “Biofactoría Sur”) in Granada (Spain).

The properties of the produced biofuel met the requirements of ISO 21640:2021 for lower heating value (LHV), chlorine content, and mercury content. According to Directive 2018/850, the waste hierarchy consists of five steps: prevention, preparation for reuse, recycling, other recovery (including energy recovery), and disposal [16]. At this point, the management of the produced SRF falls within the fourth step of the hierarchy, which pertains to “other recovery, e.g., energy recovery”. In this context, thermal routes such as combustion and gasification, which aim at the energy recovery of SRF, could be considered [17].

Combustion, also known as controlled incineration, is a process that involves the burning of some feedstock, including waste, in the presence of oxygen at temperatures between 850 and 1100 °C [18]. The primary purpose of this process is to reduce the volume and weight of the waste while recovering some of the energy contained in the waste to generate electricity, steam, or heat [19]. After incineration, atmospheric emissions and the resulting ash must be treated appropriately [20]. In combustion, controlling different operational parameters such as excess oxygen, minimum combustion temperature, and minimum residence time at minimum combustion temperature after the last air injection [21] is a key issue in the proper development of the process [22]. SRF is produced from non-hazardous solid waste components, and its composition aligns with the combustion requirements set by national and EU specifications [23], so energy recovery through combustion processes appears as an interesting alternative. Numerous studies have been conducted on the use of the SRF obtained from the non-recyclable part of municipal solid waste as fuel in combustion processes in cement kilns, lime kilns, and waste-to-energy (WtE) plants [24]. Both economic and environmental issues have been analysed, and the results confirm that this alternative could be a viable solution [25]. Currently, the thermal substitution rate of traditional fossil fuels with SRF in this type of combustion process can vary from 40% to 70% [26].

Gasification converts a carbonaceous material into a gaseous fuel by heating it in a gasification medium, typically air, oxygen, steam, or carbon dioxide (and their mixtures). Operating conditions, such as the temperature, the equivalence ratio (ER), and the gasifying agent, play a relevant role in gas composition [27], which defines its quality and potential uses in gas engines and turbines or as a chemical feedstock to produce liquid fuels [28]. The gasification of SRF from different origins, such as MSW [17] and automotive and plastics recycling industries [29], has been reported in the literature. It has also served as feed for co-gasification processes with other input streams such as wood [30], sewage sludge, or paper waste [31]. The influence of temperature and ER has been analysed in several works [32], with a general trend showing that increasing the temperature with a fixed ER implies an increase in the gas yield [33]. LHV of the gasification gas has also been the subject of study for energetic purposes [34], but unanimity on the effect of the operational parameters has not been reported; therefore, as concluded [35], LHV of the gas seems to be highly dependent on the composition of SRF.

To the best of our knowledge, there is a gap in the literature regarding the energy recovery from screening waste from WWTPs. This study builds on the successful production of SRF from this waste, in pelletised forms [14], and presents a theoretical energetic assessment (based on enthalpy balances) of two thermochemical routes, combustion and

gasification, which are potential treatments for energy recovery from SRF derived from screening waste. In addition, since information about the gasification of SRF from screening waste is scarce in the literature, the present work also provides some experimental data (product yields, syngas composition, lower heating value, and tar content) obtained in the gasification of this type of waste with air and air/steam as gasification medium. These experimental data have been used for energetic calculations in the gasification process. Complete combustion was considered in the energetic assessment of the SRF from screening waste combustion, avoiding the need for experimental data in this calculation. The findings of this study will provide a first approach to more sustainable management alternatives for this waste, involving energy recovery as opposed to the current practice of disposing of screening waste in landfills.

2. Materials and Methods

2.1. Raw Materials

The raw material considered for the experiments and energy balances was the densified SRF after drying, cleaning, crushing, and a subsequent pelletisation of screening waste [14].

Table 1 provides a brief characterisation including composition and energetic content determined according to the following standard methods: elemental analysis based on UNE-EN-ISO 21663:2021; ash according to UNE-EN ISO 21656 2021; volatiles based on UNE-EN ISO 22167:2022; LHV according to UNE-EN ISO 21654-2021; Cl content was determined in a sample of ash derived from the procedure of calorific value determination, which was diluted in distilled water, and calculated applying ion-exchange chromatography based on UNE-EN ISO 10304-1:2009; Hg content according to UNE-EN 15411:2012; and bulk density according to UNE-EN 15103:2010.

Table 1. Characterisation of pelletised solid recovered fuel (SRF) from screening waste.

Parameter (Dry Basis)	Value
C (wt%)	52.80 ± 0.4
H (wt%)	7.43 ± 0.09
N (wt%)	2.685 ± 0.007
S (wt%)	0.010 ± 0.002
O (wt%)	27.4 ± 0.5
Ash (wt%)	9.4 ± 3.4
Volatile solids (wt%)	91.0 ± 2.8
Cl (wt%)	0.3 ± 0.2
Hg (mg/MJ)	$3.8 \times 10^{-5} \pm 2.9 \times 10^{-5}$
Higher heating value (MJ/kg)	26.0 ± 2.7
Lower heating value (MJ/kg)	24.3 ± 2.6
Bulk density (kg/m ³)	58.2 ± 2.9

2.2. Gasification

2.2.1. Experimental Setup

The gasification experiments were carried out in the laboratories of the Thermochemical Processes Group (Aragón Institute of Engineering Research, I3A, of the University of Zaragoza). A laboratory-scale fluidised bed reactor was used to gasify SRF from screening waste, at atmospheric pressure. The gasifier, made of AISI 310 refractory steel, was divided into two parts: a bed zone with an inner diameter of 40 mm and a freeboard zone with an inner diameter of 63 mm. Some problems were encountered during feeding because bridging was detected in the silos due to the low density of the material, so it was decided to feed the process with SRF in pellet form. Pellets were fed manually through a double valve feeding system placed at the upper part of the reactor at a constant rate of 1.5 g/min. An electric furnace heated the reactor with three independent heating zones for the bed, freeboard, and cyclone. During the tests, the bed temperature was maintained at 800 °C,

while the cyclone temperature was kept constant at 650 °C. Calcinated dolomite, sifted at a mesh size of 500 µm, was utilised as bed material in the reactor. The experiments were carried out over 60 min to ensure the system reached a steady state.

The diagram of the gasification plant is shown in Figure 1 [36]. The gasifying agent was atmospheric air (coming from a compressor) or a mixture of air and steam. The feed rate of air was adjusted by a mass flow controller to ensure the ER required for autothermal gasification. When necessary, water was also fed through an HPLC pump; then, it was vaporised (200 °C) before mixing with the inlet air stream.

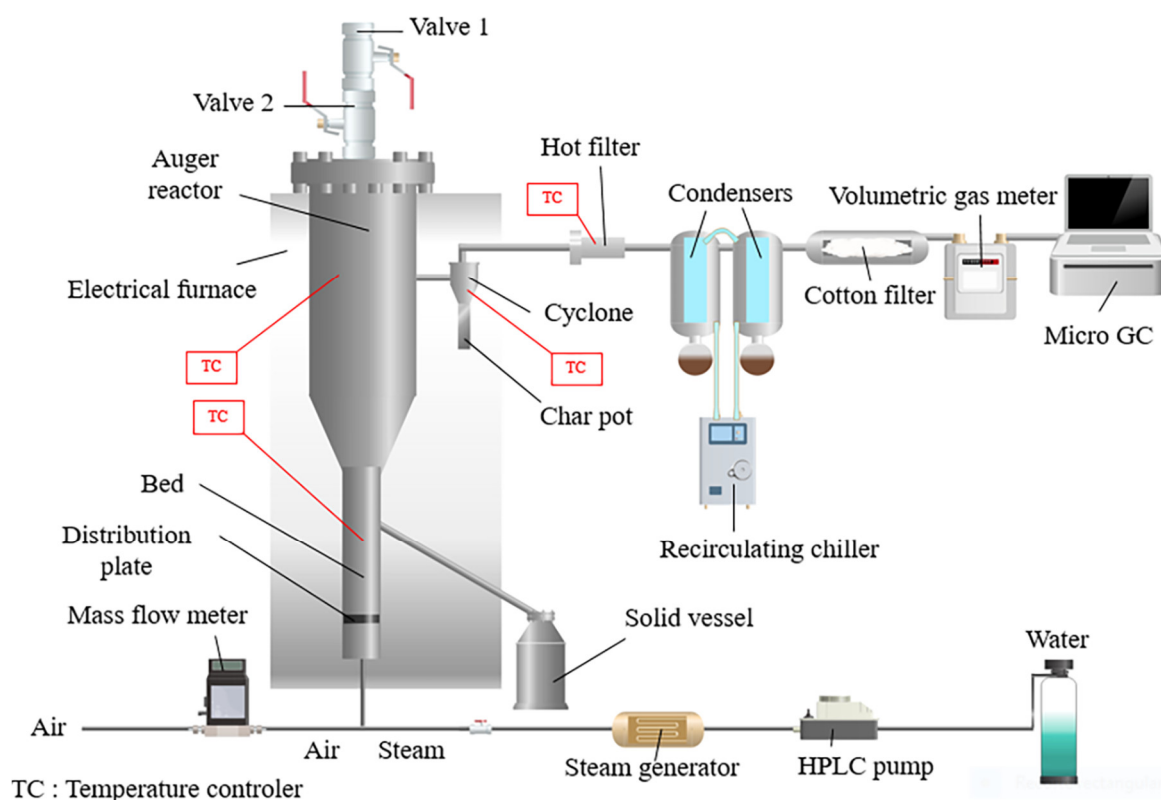


Figure 1. Scheme of the experimental gasification setup.

During the gasification process, gases were retained inside the reactor for 7 to 8 s. After this, the gas stream left the reactor dragging small solid particles, which were collected by a filtration system composed of a cyclone and the hot filter, which were maintained at a constant temperature of 650 °C and 450 °C, respectively, thus ensuring only the capture of solid particles. Then, gases and vapours produced during the process were conducted through two condensers (cooled using a water-cooled chiller) and an electrostatic precipitator. A condensed fraction composed of water and organic compounds (tar) was recovered in the condensers. Subsequently, the resulting gas was subjected to an additional filtration step using a cotton filter to remove any particles or aerosols in the gas stream.

Once the flue gas had been purified of particulates, it was volumetrically measured and, then, its composition was analysed online using a gas microchromatograph (Agilent 3000-A, Agilent, Santa Clara, CA, USA) to quantify the volumetric fraction of H₂, O₂, CO, CO₂, CH₄, C₂H₄, C₂H₆, C₂H₂, H₂S, and N₂. The composition of the gas is a consequence of several intricate reactions, among which the most significant ones are presented below:

Oxidation: $C(s) + O_2(g) \leftrightarrow CO_2(g)$	$\Delta H < 0$
Partial oxidation: $C(s) + 1/2O_2(g) \leftrightarrow CO(g)$	$\Delta H < 0$
Boudouard: $C(s) + CO_2(g) \leftrightarrow 2CO(g)$	$\Delta H > 0$
Water—gas primary: $C(s) + H_2O(g) \leftrightarrow CO(g) + H_2(g)$	$\Delta H > 0$
Water—gas secondary: $C(s) + 2H_2O(g) \leftrightarrow CO_2(g) + 2H_2(g)$	$\Delta H > 0$
Water—gas shift (WGS): $CO(g) + H_2O(g) \leftrightarrow CO_2(g) + H_2(g)$	$\Delta H < 0$
Methanation: $C(s) + 2H_2(g) \leftrightarrow CH_4(g)$	$\Delta H < 0$
Steam reforming: $C_nH_x(g) + nH_2O(g) \leftrightarrow (x/2+n)H_2(g) + nCO(g)$	$\Delta H > 0$
Dry reforming: $C_nH_x(g) + nCO_2(g) \leftrightarrow 2nCO(g) + (x/2)H_2(g)$	$\Delta H > 0$
Cracking: $C_nH_x(g) \leftrightarrow nC(s) + (x/2)H_2(g)$	$\Delta H > 0$

Finally, a Karl Fischer titration was performed to determine the amount of water present in the condensed fraction. This, in turn, allowed us to determine by difference the amount of tar present in the gas, whose composition was studied by gas chromatography coupled with mass spectrometry and flame ionisation detection. An Agilent GC/MS/FID (7890A/5975C) was used for the analyses. The most volatile fraction in the tar samples could be identified and quantified (in terms of percentage of integrated area) with this technique.

2.2.2. Experimental Design and Data Analysis

Two gasification experiments were conducted in order to estimate the influence of the gasifying medium on SRF gasification yields and gas quality. The temperature was set at 800 °C in both cases, which is a typical biomass gasification temperature. Air was used as a gasifying agent in the first test, while a mixture of air and steam was used in the second one. The ratio between the inlet mass of steam and the inlet mass of carbon contained in the SRF (which is denoted as S/C) was virtually zero in the first case (the moisture of SRF was very low as it was previously dried), while this ratio was increased up to a typical value of 1 kg steam/kg C in the second experiment by feeding steam to the reactor together with the air flow. Considering the elemental analysis of SRF and its carbon content, this S/C ratio of 1 kg steam/kg C can be converted to a steam/SRF mass ratio, obtaining a value of 0.51 kg steam/kg SRF. Therefore, these two experiments could be seen as the first approach to test the gasification of dried SRF (Test #1) and wet SRF with a moisture content of 33.7 wt% (Test #2).

The amount of air fed to the reactor is determined by the ER, which represents the percentual fraction of stoichiometric air really fed to the system. This ER was set calculating the theoretical amount of O₂ required for the autothermal gasification of SRF aiming at maintaining the temperature at 800 °C for an S/C ratio of 0 (Test #1) or 1 kg/kg (Test #2). This theoretical calculation was based on the assumption that chemical equilibrium could be reached. Adding more steam as a gasifying agent involves the occurrence of more endothermic reactions (heat demandant), so the requirement for O₂ increases to oxidise a higher fraction of the SRF and release, in turn, more heat to maintain the gasification temperature. Table 2 presents the operational conditions of the two tests performed, maintaining a temperature of 800 °C for both tests while varying the S/C ratio and the ER.

Table 2. Operational conditions in the gasification tests.

Test Number	1	2
Temperature (°C)	800	800
Steam to carbon, S/C (kg/kg)	0	1
ER (%)	29.6	37.7

The response variables analysed were the following: (i) product distribution (yields of the different gasification products: solid, gas, and tar); (ii) gas composition, determined on-line using a gas microchromatograph; (iii) LHV of the gas product (LHV_{gas}); (iv) cold gasification efficiency; (v) gas phase carbon yield; and (vi) tar composition.

The mass yields of gas, liquid, and solid products ($\eta_{m,i}$) were calculated with respect to the mass of SRF fed (Equation (1))

$$\eta_{m,i}(\text{wt}\%) = \frac{m_{\text{product}}}{m_{\text{SRF}}} \times 100 \quad (1)$$

where: m_{product} is the mass of the product (solid, gas, and tar) obtained in the reaction (kg) and m_{SRF} is the mass of SRF fed during the experiment (dry basis) (kg).

The LHV of the syngas obtained (LHV_{gas} , MJ/m³_{STP}) and the cold gas efficiency, which represents the ratio between the energy content in the produced gasification gas (cooled at room temperature) and the energy content in the solid fuel, were calculated according to Equations (2) and (3), respectively:

$$LHV_{\text{gas}} = \sum y_i \times LHV_i \quad (2)$$

where: LHV_i (MJ/m³_{STP}) is the LHV of each gaseous component and y_i is its volumetric fraction (determined with the gas microchromatograph).

$$\text{Cold gas efficiency (\%)} = \frac{LHV_{\text{gas}} \times V_{\text{gas}}}{LHV_{\text{SRF}} \times m_{\text{SRF}}} \times 100 \quad (3)$$

where: V_{gas} is the total volume of gasification gas (m³_{STP}), LHV_{SRF} (MJ/kg) is the LHV of the SRF fed, and m_{SRF} is the total mass of SRF fed during the experiment (kg).

Finally, the carbon yield to the gas phase (%) was calculated as follows:

$$\text{Carbon yield to gas phase (\%)} = \frac{m_{\text{C in gas}}}{m_{\text{C in SRF}}} \times 100 \quad (4)$$

where: $m_{\text{C in gas}}$ is the mass (g) of carbon contained in the gas product and $m_{\text{C in SRF}}$ is the mass (g) of carbon contained in the SRF.

2.3. Energy Balances

2.3.1. Thermal Drying of SRF from Screening Waste

Prior to the thermochemical treatment of the SRF by gasification or combustion, the waste must be dried. In the case of combustion, moisture content is a key factor influencing the performance of alternative fuels in incineration, including combustion completeness, energy recovery, and pollutant emission [37]. Therefore, to improve the operation and mitigate corrosion, moisture should not exceed 10 wt% [38]. In the case of the gasification, SRF was considered as a residue that had been totally dried before gasification in Test #1 (air gasification of dried SRF), while it was supposed to be a partially dried residue, with a moisture content of 33.7 wt%, in Test #2 (air/steam gasification of SRF with a ratio S/C of 1 kg steam/kg C; steam is supposed to come from the moisture of the SRF fed).

The heat requirement for drying the SRF waste (Q_{drying}) from its initial moisture (77.3 wt%) to the different final moisture contents in the range 0–10 wt% required for combustion or 0–33.7 wt% required for gasification has been calculated following an enthalpy balance, considering 100 °C as the exit temperature for SRF and steam:

$$Q_{\text{drying}} = \left(m_{\text{solids in SRF}} \times C_{p\text{SRF}} + m_{\text{H}_2\text{O in SRF}} \times C_{p\text{H}_2\text{O}(l)} \right) \cdot \Delta T + m_{\text{H}_2\text{O evap}} \times \Delta H_{\text{vap,H}_2\text{O}} \quad (5)$$

where: Q_{drying} is the heat required for drying the SRF from its original moisture (77.3 wt%) to the desired final moisture (MJ/kg of raw SRF); $m_{\text{solid in SRF}}$ is the mass of solid contained in the raw SRF (kg); $m_{\text{H}_2\text{O in SRF}}$ is the mass of water in the raw SRF before thermal drying (kg); $C_{p\text{SRF}}$ is the specific heat capacity of the dry matter in SRF, estimated as 1.6 kJ·kg⁻¹·K⁻¹; $C_{p\text{H}_2\text{O}(l)}$ is the specific heat capacity of liquid water, considered constant in the temperature interval of 298–373 K, 4.18 kJ·kg⁻¹·K⁻¹; $m_{\text{H}_2\text{O evap}}$ is the mass of water evaporated during

the thermal drying of SRF (kg); and $\Delta H_{vap,H_2O}$ is the enthalpy of vaporisation of water at the boiling point of 373 K (2.26 MJ/kg of H_2O).

2.3.2. Combustion of SRF from Screening Waste

An energy balance was carried out to predict the output gas temperature (T; Figure 2). It illustrates the combustion process of SRF. It is noted that 1 kg of dry matter in SRF, characterised by its composition, is introduced into a furnace along with 50% excess air, where combustion occurs. This thermochemical process is associated with theoretical energy losses of 15% of the input energy and yields a series of non-combustible gases, along with 9.4 wt% ash on a dry SRF basis. The analysis was based on experimental [15] and literature data [39].

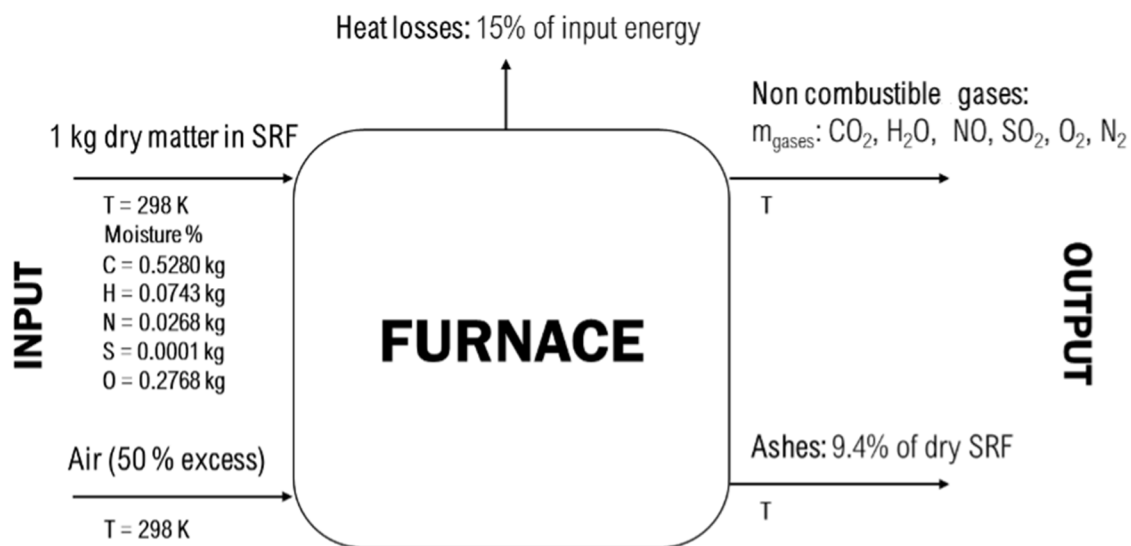


Figure 2. Combustion energy balance diagram.

The following assumptions, simplifications, and stream properties were adopted for the energy balance:

- The standard reference state was $T_0 = 25\text{ °C}$ (298 K) and $P_0 = 1.01 \times 10^5$ Pa.
- The characterisation of the input solid stream (SRF) is shown in Table 1 (dry basis).
- The calculation basis was a feeding of 1 kg of dry matter in SRF.
- Input air excess was of 50%.
- Moisture content considered in the SRF stream was varied between 0, 2.5, 5, 7.5, and 10 wt%.
- Liquid phases were considered to be ideal solutions.
- Thermodynamic properties of liquid and gaseous compounds were obtained from the literature [40].
- Heat losses (Q_{losses}) were taken into account as 15% of input energy [41].
- Combustion of the SRF was considered complete, with no unburned fuel.

Energy assessment

The enthalpy balance of the system shown in Figure 2 was performed according to Equation (6).

$$\Delta h_{input} = Q_{losses} + \Delta h_{output} \quad (6)$$

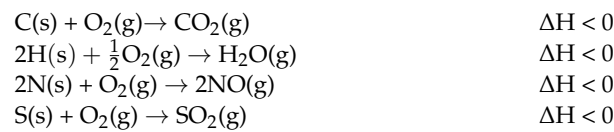
where: Q_{losses} : heat losses, which are assumed to be 15% of energy input (MJ). Δh_{input} : specific enthalpy input (MJ), which represents the sum of enthalpies of the streams entering the furnace; and Δh_{output} is the specific enthalpy output (MJ), which represents the sum of enthalpies of the streams leaving the furnace.

The enthalpy of each stream (Δh_{input} , Δh_{output}) was calculated using Equation (7).

$$\Delta h = \sum_i m_i \left(\Delta h_{f,i}^0 + \int_{T_0}^T C_{p,i} \times dT \right) \quad (7)$$

where: m_i is the mass flow of each component (considering 1 kg of dry matter in SRF as the calculation basis). Therefore, the components of the input streams are dry matter in SRF, $H_2O(l)$ in SRF (corresponding to its moisture), $O_2(g)$, and $N_2(g)$ (components of air).

The components of the output stream are gas species and ash. The gases include $CO_2(g)$, $H_2O(g)$, $NO(g)$, and $SO_2(g)$, which come from the complete combustion of the dry matter in SRF (see reactions below) and from the evaporation of the moisture content; the exit gas also includes O_2 (coming from the air excess used) and N_2 (inert). m_i values for the products were calculated by mass balances considering the elemental and ultimate analysis of SRF:



$\Delta h_{f,i}^0$: standard enthalpy of formation of each compound at the reference temperature (298 K), (MJ/kg). Data for the gases and $H_2O(l)$ involved in the process were obtained from the literature [40]. The apparent enthalpy of formation for the dry matter in SRF (feedstock) ($\Delta h_{f, dry matter in SRF}$) was calculated from its ultimate analysis and higher heating value according to Equation (8).

$$\Delta h_{f, dry matter in SRF}^0 = \left(\sum_j m_j \times \Delta h_{f,j}^0 \right) + HHV_{dry matter in SRF} \quad (8)$$

where: m_j represents the mass of each gas product derived from the complete combustion of 1 kg of dry matter in SRF under stoichiometric conditions (CO_2 , H_2O , NO , and SO_2) and $HHV_{dry matter in SRF}$ is the higher heating value of dry matter in SRF (MJ/kg), which was determined experimentally (Table 1).

$C_{p,i}$ is the average specific heat capacity of each compound in the temperature range 298–2000 K ($MJ \cdot kg^{-1} \cdot K^{-1}$). Inlet streams are considered to be at the reference temperature (298 K), so the specific heat capacity only contributes to the enthalpy balance in the product streams. The C_p of the gas components were obtained from the literature [40]. The C_p of the ash was considered constant with the temperature and equal to a typical value of $1.1 \text{ kJ} \cdot \text{kg}^{-1} \cdot \text{K}^{-1}$.

T is the temperature of the output gas, which can be calculated by solving the system of Equations (6)–(8).

Thermal energy contained in the hot gases from combustion can be recovered by generating steam in a heat exchanger. A theoretical energy balance has been performed according to Figure 3 to include this heat recovery in the process, in which the mass of steam that could be produced at 400 °C and 50 bar was calculated (kg of produced steam/kg of dry matter in SRF burnt).

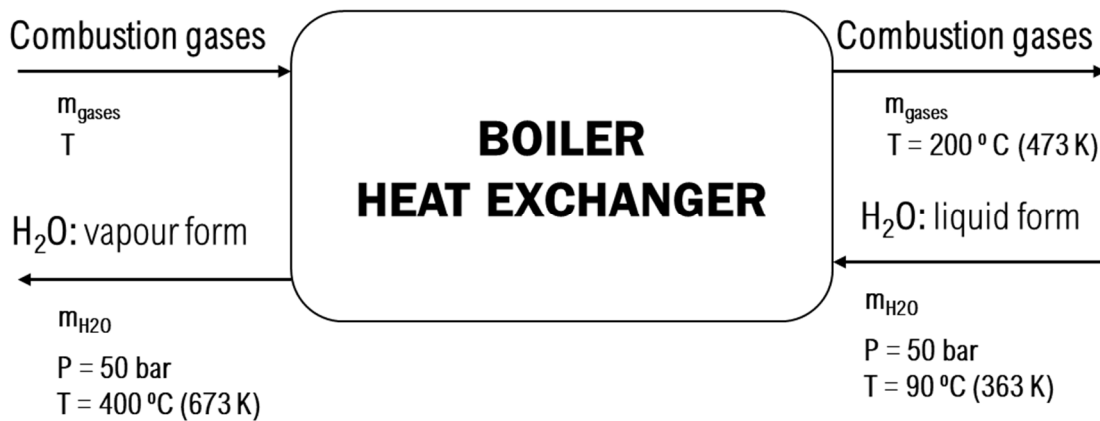


Figure 3. Heat exchanger energy balance diagram.

The following assumptions, simplifications, and stream properties were adopted for this energy balance:

- The temperature of the hot combustion gases (input stream) is the T obtained in the energy balance performed for SRF combustion (Figure 2).
- The temperature of the combustion gases at the exit of the heat exchanger (output stream) is assumed to be $200 \text{ }^\circ\text{C}$.
- A thermal efficiency (η_t) of 85% is assumed in the process [42].
- Liquid phases were considered ideal solutions.
- Thermodynamic properties of liquid and gaseous compounds were obtained from the literature [40].

The steam flow rate produced was obtained from Equation (9).

$$\eta_t \left[\sum_p m_p \times \int_{473}^T C_{p,p} dT \right] = m_{steam} \times (\Delta h_{H_2O, (50 \text{ bar}, 673 \text{ K}) (g)} - \Delta h_{H_2O, (50 \text{ bar}, 363 \text{ K}) (l)}) \tag{9}$$

where: m_p is the mass of each compound in the combustion flue gas calculated by the mass balance in the furnace (kg/kg of dry matter in SRF); $C_{p,p}$ is the average specific heat capacity of each compound in the furnace output gas stream in the temperature range $473\text{-}T \text{ K}$ ($\text{MJ}\cdot\text{kg}^{-1}\cdot\text{K}^{-1}$); m_{steam} is the mass of steam produced (kg/kg of dry matter in SRF). $\Delta h_{H_2O, (50 \text{ bar}, 673 \text{ K}) (g)}$ is the enthalpy of steam at 50 bar and 673 K (3.19 MJ/kg of steam); and $\Delta h_{H_2O, (50 \text{ bar}, 363 \text{ K}) (l)}$ is the enthalpy of liquid water at 50 bar and 363 K (0.38 MJ/kg of H_2O).

2.3.3. Gasification of SRF from Screening Waste and Combustion of the Gasification Gas

The energy assessment was based on the experimental data obtained in the gasification tests. The ER used in the experiments would theoretically allow an autothermal process ($800 \text{ }^\circ\text{C}$) in equilibrium conditions. However, as an equilibrium state is not always reached because of kinetic issues, performing an enthalpy balance with real experimental results, especially gas composition, allows an approach to the energy produced or required for the gasification tests at 1073 K under real experimental conditions (Q in Figure 4).

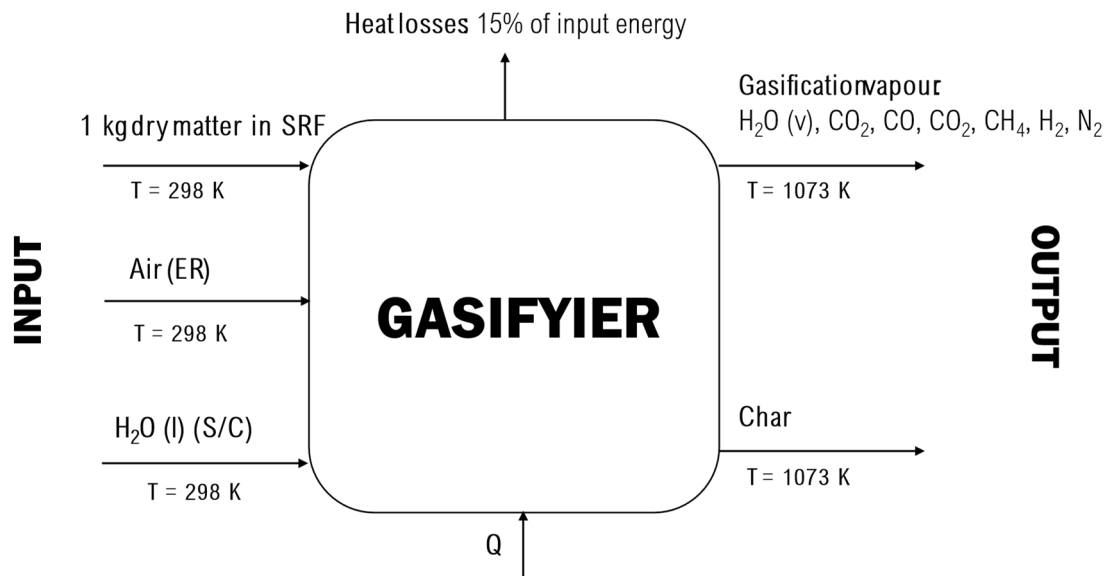


Figure 4. Gasification energy balance diagram.

The following assumptions, simplifications, and stream properties were adopted for the energy balance:

- The standard reference state was $T_0 = 25\text{ }^{\circ}\text{C}$ (298 K) and $P_0 = 1.01 \times 10^5\text{ Pa}$.
- The characterisation of the input solid stream (SRF) is shown in Table 1 (dry basis).
- The calculation basis was 1 kg of dry matter in SRF.
- The moisture content considered for the SRF stream was 0 (in Test #1) and 33.7 wt% (in Test #2).
- The tar content in the gas was considered negligible for energetic assessment.
- Char properties were considered equal to ash properties due to the high ash content.
- Heat losses were considered as 15 % of energy input [38].

Energy assessment

The enthalpy balance is expressed by Equation (10).

$$\Delta h_{input} + Q = Q_{losses} + \Delta h_{output} \quad (10)$$

where: Δh_{input} is the specific enthalpy input (MJ), which represents the sum of enthalpies of the streams entering the gasifier. Q is the heat required/produced in gasification. If the value is positive, energy is required for gasification, while energy is released if the value is negative (MJ). Q_{losses} is the heat losses (15% of input energy) (MJ). Δh_{output} is the specific enthalpy output (MJ), which represents the sum of enthalpies of the streams leaving the gasifier. The enthalpy of each stream (Δh_{input} , Δh_{output}) was calculated with Equation (7) in a similar way as was performed in the combustion process, but in this case, the composition of the gasification gas was experimentally obtained from the gasification tests, and its temperature (T) was established at 1073 K. The unknown value in this enthalpy balance was, therefore, the heat produced or required in the process (Q).

The energy contained in the gasification gas can be recovered by its combustion (Figure 5) and subsequent steam generation. A similar enthalpy energy balance to the one presented for the SRF combustion was solved by applying Equations (6)–(8) in order to calculate the temperature of the output gases obtained from the combustion of the gasification gas. The following assumptions, simplifications, and stream properties were adopted for the energy balance:

- The temperature of the gasification gas entering into the furnace was the gasification temperature $T_0 = 800\text{ }^{\circ}\text{C}$ (1073 K).
- The composition of the input stream (gasification gas) was the one obtained experimentally in the gasification tests.

- Input air excess considered was 25%.
- Combustion of the gasification gas is considered to be complete, with no unburned fuel.

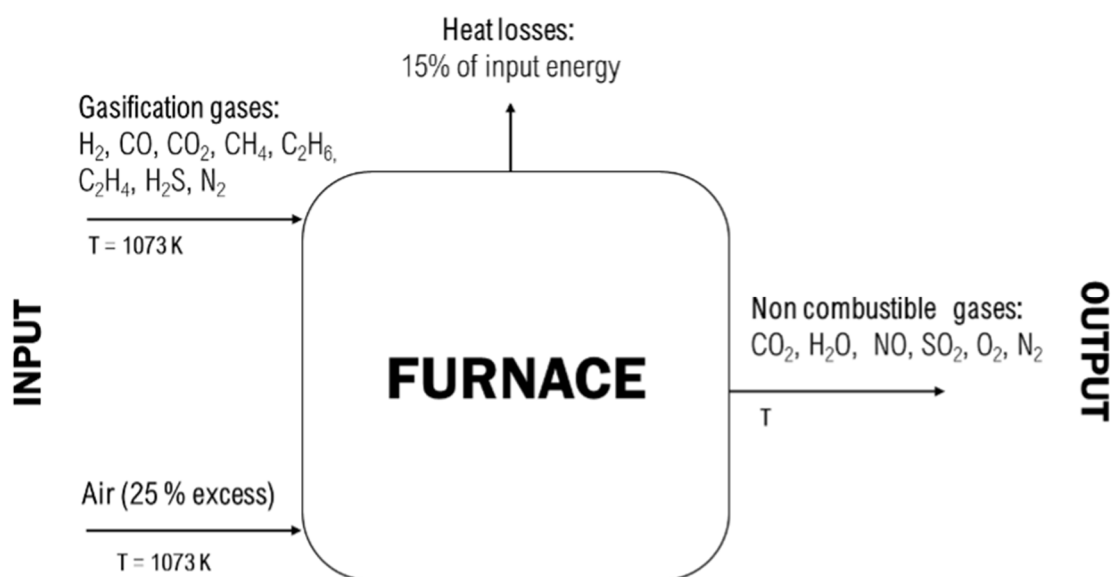


Figure 5. Energy balance diagram for the combustion of gasification gas.

The enthalpy balance is expressed by Equation (11).

$$\Delta h_{input} = Q_{losses} + \Delta h_{output} \quad (11)$$

The unknown value in this enthalpy balance for the combustion of the gasification gas was the temperature of the non-combustible gases at the exit of the furnace. Another enthalpy balance similar to the one presented in Equation (9) was performed to calculate the mass of steam generated at 50 bar and 673 K (MJ/kg of dry matter in SRF). These data are directly comparable to those obtained from the SRF combustion.

3. Results

The results are structured in three parts, corresponding to the analysis of the experimental data obtained in the SRF gasification tests, the energetic assessment of the thermochemical process proposed (drying, combustion, and gasification), and finally a comparative analysis between combustion and gasification.

3.1. SRF Gasification Trials

3.1.1. Product Yields

The mass balance closure was around 90% in both experiments (with and without steam), which is considered acceptable for the type of setup used in this work.

In alignment with prior literature [43], tests with similar operating factors have shown that the solid yield is lowered with an increase in ER. The gas yield, referring to the volume of tar-free gas produced, is higher than 100% because the gasifying agent reacts with SRF and is part of the gasification gases. The results demonstrate an inverse correlation with the solid yield, with Test #1 having the highest solid yield and the lowest gas yield. The liquid yield, which refers to the whole fraction of liquid recovered in the condensers, exhibits a similar pattern to the yield of gas, with Test #1 displaying the lowest value and Test #2 the highest one. The addition of steam as a gasifying agent in Test #2, as well as the promotion of combustion reactions because of the increased ER, could explain the production of more liquid (water specifically) under these operational conditions. Finally, the tar yield, which refers to the organic compounds present in the liquid fraction, was reduced when both S/C

and ER were increased. Reducing tar formation is a beneficial aspect of the subsequent application of the gasification gas for energy recovery.

Table 3 also illustrates the gas production from the gasification process. The results show that the gas production rate increased from 2.3 m³_{STP} gas/kg dry matter in SRF (Test #1) to 2.9 m³_{STP} gas/kg dry matter in SRF (test #2), which means an increase of 26.08%. The main reason for this increase could be the higher ER used in test #2, which also leads to a higher flow of N₂ at the inlet and exit gas [36]. Introducing more steam as a gasifying agent also promotes gasification reactions (see reactions in Section 2.2.1 of this article), thus reducing the remaining solid in favour of the production of gas. The LHV of the gas varied from 2.9 to 4.4 MJ/m³_{STP}. In contrast to the gas product flow rate, the results indicate that the best outcome for the LHV occurred at the lowest ER, corresponding to test #1, with an ER of 29.6%. As such, the LHV follows a decreasing trend concerning the ER, whose increase promotes complete oxidation reactions, thus generating more CO₂ to the detriment of the other gases.

Table 3. Gasification experimental results.

Test Number	1	2
Experiment code	T800_S/C0_ER29.6	T800_S/C1_ER37.7
Mass balance (%)	90.7	96.3
Moisture of the input SRF stream to gasification (wt%)	0	33.7
Product distribution (wt%)		
Solid yield	21.9	12.2
Liquid yield	21.6	75
Tar yield	3.6	1.4
Gas yield (N ₂ -free basis)	130.4	100.7
Gas composition (vol%, dry basis)		
H ₂	7.9	6.8
CO	9.0	4.1
CO ₂	13.3	17.8
CH ₄	3.1	2.0
C ₂ H ₆	0.2	0.1
C ₂ H ₄	2.0	1.5
H ₂ S	0.02	0.11
N ₂	63.3	67.6
H ₂ /CO molar ratio	0.874	1.66
Gas quality parameters		
Gas production (m ³ _{STP} /kg of dried SRF)	2.3	2.9
Gas LHV (MJ/m ³ _{STP}) (dry basis)	4.4	2.9
Cold gasification efficiency (%)	44.6	37.8
Gas phase carbon yield (%)	80.6	91.2
g tar/m ³ _{STP} gas	15.7	4.8

The cold gasification efficiency, which represents the ratio between the energy content of the produced gas (at room temperature) and the energy content of the solid fuel, was calculated. The cold gasification efficiency values obtained from the gasification tests ranged between 37.8% for test #2, which had the highest gas production but the lowest LHV, and 44.6% for test #1 (lower gas production but higher LHV of the gas).

3.1.2. Gas Composition

Table 3 displays the gasification gas composition for each of the conducted tests. In previous studies, the primary gases generated by gasification processes applied to biomass are H₂, CO, CO₂, and CH₄ [44]. However, for this SRF, the H₂ concentration detected accounted for only 7.9 vol% (Test #1) and 6.8 vol% (Test #2). Although a higher H₂ concen-

tration in the gas could be expected with increasing presence of steam in the gasification medium (primary water–gas reaction, secondary water–gas reaction, WGS reaction), the parallel increase in ER could be the cause of this lower production by promoting combustion reactions (including H₂ combustion) as well as the dilution of the gas components due to the higher presence of N₂. These H₂ content values were very similar to those obtained by previous studies of gasification of SRF obtained from municipal solid waste. Specifically, for a temperature of 800 °C and an S/C ratio of 0.85, a range of H₂ concentrations between 5.8 and 11.2 vol% were achieved by Pinto [30].

CO presented significant differences in both tests, with values ranging from 4.1 vol% (test #2) to 9.0 vol% (test #1). Other studies previously conducted under similar conditions [30,32,45] are consistent with the value of 9.0 vol%; however, the value of 4.1 vol% is substantially lower than the lowest value found in literature of 6.8 vol% [46].

Finally, the CO₂ content was the highest among all gases in the two tests (with the exception of N₂), reaching 17.8 vol% for Test #2 and 13.3 vol% (test #1), which shows a clear improvement in the combustion reactions. Unlike CO, in the case of CO₂, values similar to those compiled in the literature (11.66 and 15.69 vol%) were obtained during Test #2 [46]. The CH₄ concentration decreased from 3.1 vol% in Test #1 to 2.0 vol% in Test #2, obtaining in both cases values similar to those reported in the literature [32,41]. Due to the use of steam in test #2, the H₂/CO ratio presented a higher value (1.66), close to the value of 2, which is optimal for its use as syngas. However, the tar concentration was very high for any synthesis application or even for the combustion of this gas stream in a gas turbine or an engine, with direct combustion in a boiler being the most suitable application, avoiding in this way the condensation of the tar compounds.

3.1.3. Tar Composition

The tar produced during gasification is one of the critical points of the process [47], since it can cause the formation of cracks in the pores of the filters, the production of coke that clogs the filters, and the condensation and clogging of cold spots [48]. For this reason, the composition of the tar generated must be analysed to know the extent of its impact. For the present SRF gasification process, the tar was analysed by gas chromatography (GC/MS), identifying the primary compounds shown in Table 4. It is important to emphasise that the results refer to chromatographic area percentages, i.e., these percentage data do not represent the exact composition of the samples since the area/concentration response factor is different for each compound; however, these data will be very useful for comparing tar produced in different conditions.

Table 4. Gasification tar composition.

Test Number	1	2
Moisture of the input SRF stream to gasification (wt%)	0	33.7
Family of tar compounds (% of chromatographic area)		
Light aromatics with a single ring	1.5	1.7
Polycyclic aromatics	87.2	95.4
Heterocyclic aromatics containing nitrogen	7.6	0.8
Heterocyclic aromatics containing oxygen	1.4	1.5
Organic compounds containing sulfur	1.5	1.7

Based on the molecular weight of tar compounds, some researchers have divided the composition into five groups [49,50]. In this study, a similar classification of tar compounds was employed, including: (i) light aromatics with a single ring, such as styrene; (ii) polycyclic aromatic hydrocarbon compounds with two or three rings, including indene, naphthalene, n-methyl-naphthalene, biphenyl, biphenylene, fluorene, anthracene, and phenanthrene; (iii) heterocyclic aromatics containing nitrogen, such as n-methyl-pyridine, ben-

zonitrile, n-methyl-benzonitrile, quinoline, n-methyl-quinoline, indole, n-phenyl-pyridine, n-naphthalenecarbonitrile, benzoquinoline, and 5H-indeno [1,2-b]pyridine; (iv) heterocyclic aromatics containing oxygen, including phenol and benzofuran; and (v) organic compounds containing sulfur, specifically 2-benzothiophene and propanenitrile, 3,3'-thiobis-).

As seen in Table 4, the majority of compounds belong to the polycyclic aromatic group for the two experimental conditions, with 87.2% and 95.4% of chromatographic area. This difference, related to the different S/C ratio used in each experiment, is directly reflected in the group of nitrogen-containing heterocyclic aromatics, and the percentage is lower for Test #2, with 1.5%, than for Test #1, with 7.6%. The rest of the compound classification groups remain very similar for the two trials, with maximum differences of 0.2%, which are not considered significant. This composition resembles the typical one identified for tars from biomass gasification [51].

3.2. Thermal Drying

The heat required for the drying of SRF from its initial moisture (77.3 wt%) to a final moisture, between the highest moisture content considered in the SRF for its air/steam gasification (33.7 wt%) and the lowest value considered for air gasification or combustion (0 wt%), has been calculated with Equation (5) and it is shown in Figure 6 as a function of the moisture remaining in the residue after the thermal drying. Due to the high latent heat of vaporisation of water, a high heat is required for drying a wet residue. However, as the exit temperature required is not very elevated, this operation of thermal drying could be carried out in an industrial facility with residual heat streams, such as the heat contained in the combustion flue gas after the production of steam in the heat exchanger or from its own steam stream.

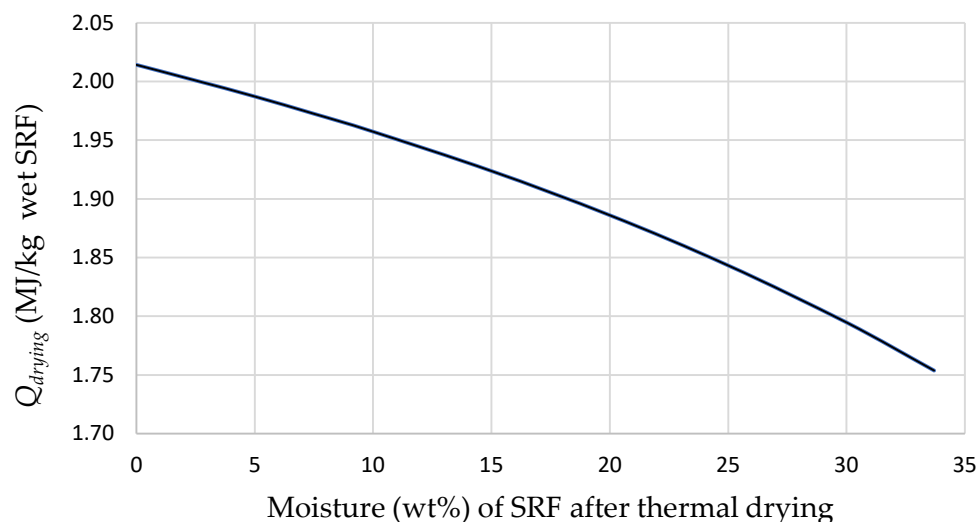


Figure 6. Heat required for drying (MJ/kg of wet SRF vs. moisture remaining in the SRF after thermal drying).

The heat required for the drying step, expressed per kilogram of dry SRF, is presented in the results section for the energy balance analyses of combustion and gasification.

3.3. Combustion

The results from the mass balance for combustion are shown in Table 5 for the different SRF initial moistures analysed in combustion: 0, 2.5, 5, 7.5, and 10 wt% (the only variation concerning the moisture is for the mass of H₂O in flue gas).

Table 5. Mass balance results of SRF combustion.

Raw SRF moisture (%) (before drying)	77.3				
Input SRF stream moisture (%) for combustion	0	2.5	5	7.5	10
Mass of combustion gases (kg/kg of dry matter in SRF)					
CO ₂	1.94	1.94	1.94	1.94	1.94
H ₂ O	0.67	0.69	0.72	0.75	0.78
NO	0.06	0.06	0.06	0.06	0.06
O ₂	0.88	0.88	0.88	0.88	0.88
N ₂	8.67	8.67	8.67	8.67	8.67
Total mass	12.21	12.24	12.27	12.29	12.32

The energy balance results according to Equations (6)–(8) are shown in Table 6. The higher the moisture content in the SRF fed to the boiler, the lower the temperature of the gases leaving the furnace, since more water should be evaporated. The values obtained for burning-temperature densified SRF from screening waste are similar to the ones obtained in the combustion of other solid residues.

Table 6. Energy balance results of SRF combustion.

Raw SRF moisture (%) (before drying)	77.3				
$\Delta h_{f,dry\ matter\ in\ SRF}^0$ (MJ/kg of dry matter in SRF)	−2.78				
Input SRF stream moisture (%)	0	2.5	5	7.5	10
Energetic terms in the combustion energy balance					
Δh_{input} (MJ/kg of dry matter in SRF)	−2.78	−3.18	−3.61	−4.06	−4.54
Heat losses (MJ/kg of dry matter in SRF)	0.42	0.48	0.54	0.61	0.68
$\sum m_i \cdot \Delta h_{f,i}^0$ (MJ/kg of dry matter in SRF)	−26.1	−26.5	−26.8	−27.2	−27.6
$\sum m_i \cdot C p_i$ (MJ/kg of dry matter in SRF)	0.024	0.024	0.025	0.025	0.025
Output T (K)	1237	1230	1222	1214	1206
Heat exchanger: amount of steam produced					
Mass of steam (kg/kg of dry matter in SRF)	5.65	5.61	5.57	5.52	5.48
Summary					
Energy recovered in the heat exchanger to produce high-pressure steam (MJ/kg of dry matter in SRF)	15.88	15.76	15.65	15.51	15.40
Drying energy (MJ/kg of dry matter in SRF)	8.85	8.81	8.77	8.68	8.63
Final energy benefit (MJ/kg of dry matter in SRF)	7.03	6.95	6.88	6.83	6.77

The energy in the flue gases can be recovered, producing steam at 673 K and 50 bar, which can be used in the WWTP. Table 6 displays the amount of steam generated per kilogram of dry matter in SRF. Although a higher amount of steam is produced when burning totally dried SRF, higher energy is also required during the drying step.

The final energy benefit after the combustion process (Table 6) can be calculated by subtracting the energy required for drying from the energy recovered in the heat exchanger to produce high-pressure steam at 50 bar and 673 K. The results showed that the initial moisture of the SRF fed to the boiler in the analysed range (0–10 wt%) slightly affects to the energy benefit, with the highest value being the one obtained for the SRF that was totally dried. Approximately 7 MJ could be recovered from the combustion of 1 kg of dry matter in SRF, which corresponds to 1.6 MJ per kg of raw SRF with 77.3 wt% moisture (before drying). This energy benefit could be even higher if the combustion gas stream after steam generation, still at 473 K, could be used for partially drying the SRF.

3.4. Gasification

According to the procedure explained in Section 2.3.3 (Equation (10)), the heat generated or required in the gasification process has been calculated (Q) and displayed in Table 7. The values obtained indicate that, considering the gasification gas composition obtained experimentally (Table 5) and 15% heat losses in the gasifier, air gasification of dry SRF with an ER = 0.296 at 800 °C is an exothermic process (negative value for Q), but air/steam gasification with S/C = 1 and ER = 0.377 is endothermic (positive value for Q). These results suggest that air gasification of dry SRF at 800 °C could be performed with a lower ER than 0.296, which would improve the gas quality, but air/steam gasification would require higher ER to be autothermal, which would result in poorer gas quality. This important difference in the enthalpy balance of the gasification among both conditions arises from the important difference in the enthalpy of the feedstock, caused by the significant feed of liquid water to the system. Therefore, to improve the enthalpy balance and obtain an autothermal process, reducing moisture in the input SRF stream is another possible option for the gasification route.

Table 7. Energy balance results for gasification trials.

Test Number	1	2
Experiment code	T800_S/C0_ER29.6	T800_S/C1_ER37.7
Moisture of the input SRF stream to gasification (%)	0	33.7
Energetic assessment in gasification trials		
Δh_{input} (MJ/kg of dry matter in SRF)	−2.78	−10.87
Δh_{output} (MJ/kg of dry matter in SRF)	−6.21	−8.64
Q (MJ/kg of dry matter in SRF)	−3.43	2.23

Combustion of the gasification gas and subsequent steam generation allows energy recovery from the gasification process. The enthalpy balance developed for this process is similar to the one carried out for the SRF combustion (Section 3.2). Tables 8 and 9 show, respectively, the mass and energy balance results for the combustion of the gasification gas obtained from air and air/steam gasification experiments. As commented before, 1 kg of dry SRF fed to the gasifier has been considered as the calculation basis for mass and energy balances.

The temperature of the flue gas produced in the combustion of the syngas from air gasification is higher than the one from the combustion of the gas stream produced in air/steam gasification, because although the amount of gases generated during air gasification is lower, its LHV is much higher.

The results obtained for the enthalpy balance in the gasification process and in a heat exchanger are presented in Table 9. The energy recovered to produce high-pressure steam in the heat exchanger is directly related to the amount of hot flue gas entering the exchanger and its temperature. The flue gas temperature was significantly higher when syngas from air gasification was burned (2112 °C) than when burning the syngas from air/steam gasification (1647 °C). Therefore, the high-pressure steam production rate was higher in the first case (4.12 vs. 3.53 kg/kg dry matter in SRF), and, in turn, more enthalpy was recovered as high-pressure steam when the fuel gas was produced by air gasification instead of air/steam gasification. Furthermore, air gasification was found to be an exothermic process ($Q = -3.43$ MJ), while air/steam gasification was found to be endothermic ($Q = +2.23$ MJ), so these energy terms should be considered to calculate the final energy that could be recovered from the entire process. In the first case, the total thermal energy recovered is the sum of the high-pressure enthalpy and the heat released during air gasification, while in the second case the energy required for air/steam gasification must be subtracted from high-pressure enthalpy. Finally, by subtracting the energy required for SRF drying, the final net energy benefit can be obtained.

Table 8. Mass balance results of gasification gas combustion.

Test Number	1	2
Experiment code	T800_S/C0_ER29.6	T800_S/C1_ER37.7
Moisture of the input SRF stream to gasification (%)	0	33.7
Gasification gas composition (kg/kg of dry matter in SRF)		
H ₂	0.017	0.018
CO	0.263	0.151
CO ₂	0.612	1.03
CH ₄	0.051	0.041
C ₂ H ₆	0.005	0.003
C ₂ H ₄	0.057	0.056
H ₂ S	0.0007	0.0049
H ₂ O	0.216	0.75
N ₂	1.85	2.49
Air flow fed to the furnace		
Excess above stoichiometric (%)		25
O ₂ (kg/kg of dry matter in SRF)	0.883	0.761
N ₂ (kg/kg of dry matter in SRF)	2.91	2.51
Calculation of generated output gases (kg/kg of dry matter in SRF)		
CO ₂	1.36	1.56
H ₂ O	0.566	1.08
O ₂	0.177	0.152
N ₂	4.76	4.99
Total mass	6.86	7.80

Table 9. Energy balance results for gasification gas combustion.

Test Number	1	2
Experiment code	T800_S/C0_ER29.6	T800_S/C1_ER37.7
Moisture of the input SRF stream to gasification (%)	0	33.7
Energetic terms in the gasification energy balance		
Δh_{input} (MJ/kg of dry matter in SRF)	−4.38	−13.5
Heat losses (MJ/kg of dry matter in SRF)	0.656	2.03
$\sum m_i \cdot \Delta h_{f,i}^0$ (MJ/kg of dry matter in SRF)	−19.79	−28.62
$\sum m_i \cdot C p_i$ (MJ/kg of dry matter in SRF)	0.0081	0.0097
Output T (K)	2112	1647
Heat exchanger: amount of steam produced		
Mass of steam (kg/kg of dry matter in SRF)	4.12	3.53
Summary		
Energy recovered in the heat exchanger to produce high-pressure steam (MJ/kg of dry matter in SRF)	11.58	9.92
Total energy recovered after gasification and heat exchanger (MJ/kg of dry matter in SRF)	15.01	7.69
Drying energy (MJ/kg of dry matter in SRF)	8.85	7.73
Final energy benefit (MJ/kg of dry matter in SRF)	6.16	−0.04

In summary, the results suggest that both air gasification (gasifying totally dried material) and combustion (up to 10 wt% moisture) allow recovering net energy from wet SRF. On the other hand, the entire process including air/steam gasification of SRF as the main step has resulted in an autothermal process, which does not seem useful for energetic purposes.

3.5. Comparative Analysis: Gasification vs. Combustion

When comparing gasification and combustion of SRF, it is important to consider both the energy efficiency and the environmental implications of each technique. According to the energy balance results, SRF combustion demonstrates superiority in terms of energy efficiency. When burning completely dried SRF, combustion allows recovering up to 1.6 MJ per kg of processed wet SRF (with initial moisture content of 77.3 wt% before drying), while air gasification allows of around 1.4 MJ per kg of wet SRF. This performance is consistent with the results shown in previous studies found in the literature concerning the combustion of SRF in facilities such as WtE plants or cement kilns, in which energy benefits close to 1.8 MJ per kg of processed SRF have been reported, depending on operational conditions and the specific type of SRF used [24,25]. On the other hand, the energy benefit obtained in this study for the air gasification of dried SRF (1.6 MJ/kg of processed SRF) is slightly higher and comparable to those found in the literature for the co-gasification of SRF (produced from different residues) with biomass or plastic wastes (0.5–0.6 MJ/kg) [30,52]. Such differences may be attributed to variations in SRF composition, gasifier characteristics, and operational conditions, such as the equivalence ratio or the gasification temperature. In contrast, SRF air/steam gasification, under the operating conditions set in this study, does not seem to be a useful process for energy recovery, as the energy balance of the entire process resulted in an energy benefit of 0 MJ. Analysing the product yields and energetic efficiency of air/steam gasification when feeding SRF with lower moisture content could be an interesting work to explore.

From an energy efficiency standpoint, SRF combustion represents the most effective option and is suitable for applications where maximising the recovered energy is the primary objective. However, air gasification, while less efficient in terms of recovered energy, offers substantial benefits regarding sustainability and potential for integrating cleaner technologies. Therefore, gasification is preferable in contexts where emission reduction and integration with renewable energy sources are critical. Recent studies highlight that gasification, as a partially oxidative process, produces a synthesis gas that, while less energetic compared to combustion, has a lower direct environmental impact [17,27]. This aligns with previous studies that highlight gasification as a viable and preferable alternative in scenarios where sustainability and emission reduction are priorities, despite its lower intrinsic energy efficiency [35]. Consequently, the choice between combustion or gasification should be informed by a comprehensive analysis that considers not only immediate energy efficiency but also long-term sustainability and adaptability to future energy and environmental requirements.

4. Conclusions

This paper analyses the possible application of thermochemical processes (combustion and gasification) for valorisation of the SRF obtained from screening waste from a WWTP. After studying these alternatives, this paper makes the following conclusions:

- Valorisation of SRF derived from screening wastes by means of gasification would be feasible. Experimental tests at the laboratory scale have demonstrated the technical feasibility of the process. The gasification gas obtained reached up to 4.4 MJ/m³_{STP}, but its high tar content makes it suitable only for direct use in boilers. Air/steam gasification, under the conditions used in this study, resulted in a gas with lower tar content than air gasification, but its LHV would not allow burning it without the aid of an auxiliary fuel.
- From an energy point of view, combustion, with energy benefits of up to 1.6 MJ per kg of wet raw SRF (with 77.3% of moisture), proved to be a more efficient process than gasification, which achieved a maximum benefit of 1.4 MJ per kg of wet raw SRF when gasifying the totally dried SRF with only air as a gasifying agent.

Author Contributions: Conceptualisation, M.Z. and G.G.; methodology, M.Z. and J.J.d.l.T.-B.; software, M.Z.; validation, J.M.-P. and I.F.; formal analysis, J.J.d.l.T.-B.; investigation, J.J.d.l.T.-B.; resources, N.G.-L.; data curation, J.M.-P.; writing—original draft preparation, J.J.d.l.T.-B. and J.M.-P.; writing—review and editing, J.J.d.l.T.-B. and J.M.-P.; visualisation, M.Z. and G.G.; supervision, G.G. and J.M.-P.; project administration, M.Z. and J.C.T.-R.; funding acquisition, J.C.T.-R. and I.F. All authors have read and agreed to the published version of the manuscript.

Funding: This work was supported by EMASAGRA S.A. (research project No. 4325 Valorización energética de residuos de desbaste como combustible sólido recuperado para lograr el residuo cero en EDAR).

Institutional Review Board Statement: Not applicable.

Informed Consent Statement: Not applicable.

Data Availability Statement: Data is contained within the article.

Acknowledgments: The authors express gratitude for providing frame support for this work to the Project PID2022-137016OB-I00 financed by Ministerio de Ciencia, Innovación y Universidades and Agencia Estatal de Investigación (MICIU/AEI)/10.13039/501100011033, Spain and by FEDER, UE. The Aragón Government has also given frame support (Research Group Ref. T22_23R). I. Fonts acknowledges the post-doctoral fellowship (RYC2020-030593-I) financed by MICIU/AEI/10.13039/501100011033 and by El FSE invierte en tu futuro.

Conflicts of Interest: The authors declare that they have no known competing financial interests or personal relationships that could have appeared to influence the work reported in this paper. Juan Carlos Torres-Rojo is employee of Emasagra S.A., who provided funding and technical support for the work.

References

1. Raheem, A.; Sikarwar, V.S.; He, J.; Dastyar, W.; Dionysiou, D.D.; Wang, W.; Zhao, M. Opportunities and challenges in sustainable treatment and resource reuse of sewage sludge: A review. *Chem. Eng. J.* **2018**, *337*, 616–641. [CrossRef]
2. Moreno-García, A.F.; Neri-Torres, E.E.; Mena-Cervantes, V.Y.; Altamirano, R.H.; Pineda-Flores, G.; Luna-Sánchez, R.; García-Solares, M.; Vazquez-Arenas, J.; Suastes-Rivas, J.K. Sustainable biorefinery associated with wastewater treatment of Cr (III) using a native microalgae consortium. *Fuel* **2021**, *290*, 119040. [CrossRef]
3. Ballesteros, I.; Duque, A.; Negro, M.; Coll, C.; Latorre-Sánchez, M.; Hereza, J.; Iglesias, R. Valorisation of cellulosic rejections from wastewater treatment plants through sugar production. *J. Environ. Manag.* **2022**, *312*, 114931. [CrossRef] [PubMed]
4. Boni, M.R.; Poletini, A.; Pomi, R.; Rossi, A.; Filippi, A.; Cecchini, G.; Frugis, A.; Leoni, S. Valorisation of residues from municipal wastewater sieving through anaerobic (co-)digestion with biological sludge. *Waste Manag. Res.* **2021**, *40*, 814–821. [CrossRef]
5. Hyaric, R.L.E.; Naquin, P.; Barillon, B.; Canler, J.-P.; Gourdon, R. Characterization of screenings from municipal wastewater treatment plants in the Region Rhône-Alpes. *Water Sci Technol.* **2009**, *60*, 25–31. [CrossRef] [PubMed]
6. Wid, N.; Horan, N.J. Anaerobic digestion of screenings for biogas recovery. *Green Energy Technol.* **2018**, 85–103. [CrossRef]
7. Cadavid-Rodriguez, L.S.; Horan, N. Reducing the environmental footprint of wastewater screenings through anaerobic digestion with resource recovery. *Water Environ. J.* **2012**, *26*, 301–307. [CrossRef]
8. Le, R.; Canler, J.-P.; Barillon, B.; Naquin, P.; Gourdon, R. Pilot-scale anaerobic digestion of screenings from wastewater treatment plants. *Bioresour. Technol.* **2010**, *101*, 9006–9011. [CrossRef]
9. Tsiakiri, E.P.; Mpougali, A.; Lemonidis, I.; Tzenos, C.A.; Kalamaras, S.D.; Kotsopoulos, T.A.; Samaras, P. Estimation of energy recovery potential from primary residues of four municipal wastewater treatment plants. *Sustainability* **2021**, *13*, 7198. [CrossRef]
10. Dong, L.; Qi, W.; Sun, Y. Semi-Dry Mesophilic Anaerobic Digestion of Water Sorted Organic Fraction of Municipal Solid Waste (WS-OFMSW). *Bioresour. Technol.* **2010**, *101*, 2722–2728. [CrossRef]
11. Casado, R.R.; Rivera, J.A.; García, E.B.; Cuadrado, R.E.; Llorente, M.F.; Sevillano, R.B.; Delgado, A.P. Classification and characterisation of SRF produced from different flows of crossMark of processed MSW in the Navarra region and its co-combustion performance with olive tree pruning residues. *WASTE Manag.* **2016**, *47*, 206–216. [CrossRef] [PubMed]
12. Sprenger, C.J.; Tabil, L.G.; Soleimani, M.; Agnew, J.; Harrison, A. Pelletization of Refuse-Derived Fuel Fluff to Produce High Quality Feedstock. *J. ENERGY Resour. Technol. ASME* **2018**, *140*, 042003. [CrossRef]
13. AENOR. Norma Española 21640:2021 Combustibles Sólidos Recuperados Especificaciones y Clases. 2021. Available online: <https://tienda.aenor.com/norma-une-en-iso-21640-2021-n0068001> (accessed on 20 June 2023).
14. De la Torre-Bayo, J.J.; Zamorano, M.; Torres-Rojo, J.C.; Rodríguez, M.L.; Martín-Pascual, J. Analyzing the production, quality, and potential uses of solid recovered fuel from screening waste of municipal wastewater treatment plants. *Process Saf. Environ. Prot.* **2023**, *172*, 950–970. [CrossRef]
15. De la Torre-Bayo, J.J.; Martín-Pascual, J.; Torres-Rojo, J.C.; Zamorano, M. Characterization of screenings from urban wastewater treatment plants: Alternative approaches to landfill disposal. *J. Clean. Prod.* **2022**, *380*, 134884. [CrossRef]

16. European Parliament and Council. Directive (EU) 2018/850 of the European Parliament and of the Council of 30 May 2018 amending Directive 1999/31/EC on the landfill of waste. *Off. J. Eur. Union* **2018**, *2018*, 100–108. Available online: <https://eur-lex.europa.eu/legal-content/EN/TXT/PDF/?uri=CELEX:32018L0850&from=EN> (accessed on 22 June 2023).
17. Al-Moftah, A.M.S.H.; Marsh, R.; Steer, J. Life cycle assessment of solid recovered fuel gasification in the state of qatar. *ChemEngineering* **2021**, *5*, 81. [[CrossRef](#)]
18. Edo-Alcón, N.; Gallardo, A.; Colomer-Mendoza, F.J.; Edo-Alcon, N.; Gallardo, A.; Colomer-Mendoza, F.J. Characterization of SRF from MBT plants: Influence of the input waste and of the processing technologies. *FUEL Process. Technol.* **2016**, *153*, 19–27. [[CrossRef](#)]
19. Karlsson, S.; Amand, L.-E.; Liske, J. Reducing high-temperature corrosion on high- alloyed stainless steel superheaters by co-combustion of municipal sewage sludge in a fluidised bed boiler. *FUEL* **2015**, *139*, 482–493. [[CrossRef](#)]
20. Wu, H.; Glarborg, P.; Frandsen, F.J.; Dam-Johansen, K.; Jensen, P.A.; Sander, B. Trace elements in co-combustion of solid recovered fuel and coal. *FUEL Process. Technol.* **2013**, *105*, 212–221. [[CrossRef](#)]
21. Vainio, E.; Yrjas, P.; Zevenhoven, M.; Brink, A.; Laurén, T.; Hupa, M.; Kajolinna, T.; Vesala, H. The fate of chlorine, sulfur, and potassium during co-combustion of bark, sludge, and solid recovered fuel in an industrial scale BFB boiler. *FUEL Process. Technol.* **2013**, *105*, 59–68. [[CrossRef](#)]
22. Lombardi, L.; Carnevale, E.; Corti, A. A review of technologies and performances of thermal treatment systems for energy recovery from waste. *Waste Manag.* **2015**, *37*, 26–44. [[CrossRef](#)]
23. Gerassimidou, S.; Velis, C.A.; Williams, P.T.; Castaldi, M.J.; Black, L.; Komilis, D. Technology Chlorine in waste-derived solid recovered fuel (SRF), co-combusted in cement kilns: A systematic review of sources, reactions, fate and implications. *Crit. Rev. Environ. Sci. Technol.* **2020**, *51*, 140–186. [[CrossRef](#)]
24. Conesa, J.A.; Rey, L.; Egea, S.; Rey, M.D. Pollutant Formation and Emissions from Cement Kiln Stack Using a Solid Recovered Fuel from Municipal Solid Waste. *Environ. Sci. Technol.* **2011**, *45*, 5878–5884. [[CrossRef](#)] [[PubMed](#)]
25. Reza, B.; Soltani, A.; Ruparathna, R.; Sadiq, R.; Hewage, K. Environmental and economic aspects of production and utilization of RDF as alternative fuel in cement plants: A case study of Metro Vancouver Waste Management. *Resour. Conserv. Recycl.* **2013**, *81*, 105–114. [[CrossRef](#)]
26. Saveyn, H.; Eder, P.; Thonier, G.; Hestin, M. Towards a better exploitation of the technical potential of waste- to-energy. In *EUR 28230 EN*; Publications Office of the European Union: Luxembourg, 2016; ISBN 978-92-79-63778-0.
27. Santamaria, L.; Beirrow, M.; Mangold, F.; Lopez, G.; Olazar, M.; Schmid, M.; Li, Z.; Scheffknecht, G. Influence of temperature on products from fluidized bed pyrolysis of wood and solid recovered fuel. *Fuel* **2021**, *283*, 118922. [[CrossRef](#)]
28. McKendry, P. Energy production from biomass (Part 3): Gasification technologies. *Bioresour. Technol.* **2002**, *83*, 55–63. [[CrossRef](#)]
29. Vonk, G.; Piriou, B.; Wolbert, D.; Cammarano, C.; Vaitilingom, G. Analysis of pollutants in the product gas of a pilot scale downdraft gasifier fed with wood, or mixtures of wood and waste materials. *Biomass Bioenergy* **2019**, *125*, 139–150. [[CrossRef](#)]
30. Pinto, F.; André, R.N.; Carolino, C.; Miranda, M.; Abelha, P.; Direito, D.; Perdikaris, N.; Boukis, I. Gasification improvement of a poor quality solid recovered fuel (SRF). Effect of using natural minerals and biomass wastes blends. *Fuel* **2014**, *117*, 1034–1044. [[CrossRef](#)]
31. Akkache, S.; Hernandez, A.-B.; Teixeira, G.; Gelix, F.; Roche, N.; Ferrasse, J.H. Co-gasification of wastewater sludge and different feedstock: Feasibility study. *Biomass Bioenergy* **2016**, *89*, 201–209. [[CrossRef](#)]
32. Recari, J.; Berruenco, C.; Abelló, S.; Montané, D.; Farriol, X. Gasification of two solid recovered fuels (SRFs) in a lab-scale fluidized bed reactor: Influence of experimental conditions on process performance and release of HCl, H₂S, HCN and NH₃. *Fuel Process. Technol.* **2016**, *142*, 107–114. [[CrossRef](#)]
33. Arena, U.; Di Gregorio, F. Fluidized bed gasification of industrial solid recovered fuels. *WASTE Manag.* **2016**, *50*, 86–92. [[CrossRef](#)] [[PubMed](#)]
34. Dunnu, G.; Panopoulos, K.; Karellas, S.; Maier, J.; Toulidou, S.; Koufodimos, G.; Boukis, I.; Kakaras, E. The solid recovered fuel Stabilat (R): Characteristics and fluidised bed gasification tests. *Fuel* **2012**, *93*, 273–283. [[CrossRef](#)]
35. Hervy, M.; Remy, D.; Dufour, A.; Mauviel, G. Air-blown gasification of Solid Recovered Fuels (SRFs) in lab-scale bubbling fluidized-bed: Influence of the operating conditions and of the SRF composition. *ENERGY Convers. Manag.* **2019**, *181*, 584–592. [[CrossRef](#)]
36. Afailal, Z.; Gil-Lalaguna, N.; Fonts, I.; Gonzalo, A.; Arauzo, J.; Sánchez, J.L. Thermochemical valorization of argan nutshells: Torrefaction and air-steam gasification. *Fuel* **2023**, *332*, 125970. [[CrossRef](#)]
37. Xiao, Z.; Yuan, X.; Jiang, L.; Chen, X.; Li, H.; Zeng, G.; Leng, L.; Wang, H.; Huang, H. Energy recovery and secondary pollutant emission from the combustion of co-pelletized fuel from municipal sewage sludge and wood sawdust. *Energy* **2015**, *91*, 441–450. [[CrossRef](#)]
38. Xu, J.; Sun, Y.; Liu, Y.; Yuan, W.; Dai, L.; Xu, W.; Wang, H. In-situ sludge settleability improvement and carbon reuse in SBR process coupled with hydrocyclone. *Sci. Total Environ.* **2019**, *69*, 133825. [[CrossRef](#)]
39. Abedin, M.J.; Masjuki, H.H.; Kalam, M.A.; Sanjid, A.; Rahman, S.M.A.; Masum, B.M. Energy balance of internal combustion engines using alternative fuels. *Renew. Sustain. Energy Rev.* **2013**, *26*, 20–33. [[CrossRef](#)]
40. Perry, R.H.; Green, D.W.; Maloney, J. *Perry's Chemical Engineers' Handbook*; McGraw-Hill B: New York, NY, USA, 1998.
41. Manganaro, J.; Chen, B.; Adeosun, J.; Lakhapatri, S.; Favetta, D.; Lawal, A.; Farrauto, R.; Dorazio, L.; Rosse, D.J. Conversion of Residual Biomass into Liquid Transportation Fuel: An Energy Analysis. *Energy Fuels* **2011**, *25*, 2711–2720. [[CrossRef](#)]

42. Chowdhury, J.I.; Hu, Y.; Haltas, I.; Balta-Ozkan, N.; Matthew, G.J.; Varga, L. Reducing industrial energy demand in the UK: A review of energy efficiency technologies and energy saving potential in selected sectors. *Renew. Sustain. Energy Rev.* **2018**, *94*, 1153–1178. [[CrossRef](#)]
43. Chiang, K.-Y.; Lu, C.-H.; Lin, M.-H.; Chien, K.-L. Reducing tar yield in gasification of paper-reject sludge by using a hot-gas cleaning system. *Energy* **2013**, *50*, 47–53. [[CrossRef](#)]
44. Gil-Lalaguna, N.; Sánchez, J.L.; Murillo, M.B.; Gea, G. Use of sewage sludge combustion ash and gasification ash for high-temperature desulphurization of different gas streams. *Fuel* **2015**, *141*, 99–108. [[CrossRef](#)]
45. Siedlecki, M.; De Jong, W. Biomass gasification as the first hot step in clean syngas production process e gas quality optimization and primary tar reduction measures in a 100 kW thermal input steam e oxygen blown CFB gasifier. *Biomass Bioenergy* **2011**, *35*, S40–S62. [[CrossRef](#)]
46. Arena, U.; Di Gregorio, F. Corrigendum to Gasification of a solid recovered fuel in a pilot scale fluidized bed reactor [117 (2013) 528–536]. *Fuel* **2014**, *120*, 528–536. [[CrossRef](#)]
47. Anis, S.; Zainal, Z.A. Tar reduction in biomass producer gas via mechanical, catalytic and thermal methods: A review. *Renew. Sustain. Energy Rev.* **2011**, *15*, 2355–2377. [[CrossRef](#)]
48. Corella, J.; Orío, A.; Aznar, P. Biomass Gasification with Air in Fluidized Bed: Reforming of the Gas Composition with Commercial Steam Reforming Catalysts. *Ind. Eng. Chem. Res.* **1998**, *37*, 4617–4624. [[CrossRef](#)]
49. Li, C.; Suzuki, K. Tar property, analysis, reforming mechanism and model for biomass gasification-An overview. *Renew. Sustain. Energy Rev.* **2009**, *13*, 594–604. [[CrossRef](#)]
50. Ponzio, A.; Kalisz, S.; Blasiak, W. Effect of operating conditions on tar and gas composition in high temperature air/steam gasification (HTAG) of plastic containing waste. *Fuel Process. Technol.* **2006**, *87*, 223–233. [[CrossRef](#)]
51. Coll, R.; Salvadó, J.; Farriol, X.; Montané, D. Steam reforming model compounds of biomass gasification tars: Conversion at different operating conditions and tendency towards coke formation. *Fuel Process. Technol.* **2001**, *74*, 19–31. [[CrossRef](#)]
52. Vonk, G.; Piriou, B.; Santos, P.F.D.; Wolbert, D.; Vaitilingom, G. Comparative analysis of wood and solid recovered fuels gasification in a downdraft fixed bed reactor. *Waste Manag.* **2019**, *85*, 106–120. [[CrossRef](#)]

Disclaimer/Publisher’s Note: The statements, opinions and data contained in all publications are solely those of the individual author(s) and contributor(s) and not of MDPI and/or the editor(s). MDPI and/or the editor(s) disclaim responsibility for any injury to people or property resulting from any ideas, methods, instructions or products referred to in the content.